

LIQUID PHASE DISPERSION/MIXING INVESTIGATION IN GAS-LIQUID UPFLOW MOVING BED HYDROTREATER REACTOR (MBR) USING DEVELOPED LIQUID TRACER TECHNIQUE AND METHOD BASED ON CONVOLUTION REGRESSION AND WAVE MODEL

Vineet Alexander¹, Hamza Albazzaz², Muthanna Al-Dahhan^{*,3}

^{1,*}*Department of Chemical & Biochemical Engineering, Missouri University of Science and Technology, Rolla, MO-65409*

²*Kuwait Institute for Scientific Research, Safat, Kuwait*

³*Cihan University, Erbil, Iraq*

Email: ¹vineet.alexander@gmail.com, ^{,3}aldahhanm@mst.edu*

Abstract

Liquid phase dispersion/mixing studies have been performed for the first time on the catalyst bed of a cold flow scaled-down upflow moving bed reactor (MBR) using residence time distribution (RTD) at various flow rates including the scaled down condition. MBR is hydrotreater and its design includes catalyst bed with conical bottom and plenum. The catalyst bed is modeled using Wave Model, and its mixing parameters are estimated using a mathematical approach based on convolution and regression. A study is also shown to illustrate the limitation of Axial Dispersion Model (ADM) while modeling the flow which noticeably deviates from plug flow. In addition, a

dimensionless variance is also estimated for the bed region from the RTDs. Overall liquid dispersion/mixing is seen high in MBR, with more dispersion/mixing in the expanded bed region. Scaled down conditions are seen best when considering the overall catalyst utilization and liquid mixing for hydrotreatment.

Keywords: Residence Time Distribution (RTD), Wave Model (WM), Moving Bed Reactor (MBR), Liquid Tracer, Liquid Dispersion Coefficient, Peclet Number, Axial Dispersion Model (ADM)

1. Introduction

Gas-Liquid-Solid reactors are widely used for industrial processes and are designed according to the hydrodynamics, heat, and mass transfer requirements of the process [1]. Two-phase upflow fixed bed reactors are used for hydrotreatment applications, as it satisfies the principal design requirement of hydrotreatment process which is to provide desired gas to liquid flow ratio, the low residence time of liquid, better liquid distribution, and fully wetted catalyst along the length of the reactor [[2], [3]]. Although, the two-phase upflow fixed bed design provides a good working condition for hydrotreatment applications, but it could fail in the proper handling of the hydrocarbon feed with a high level of contaminants. As at hydrotreatment condition of temperature around 400-410°C and pressure of 100-200 bar [3] the contaminants of crude oil deactivates catalyst fast and results in the frequent shutdown of the reactor for catalyst replacement. Ebullated bed technology, which

15 is upflow gas-liquid over liquid fluidized bed [3] with provision for catalyst
16 replacement, is used for handling heavier crude oil feed. As the catalyst re-
17 placement enables reactor to run continuously without frequent shutdown,
18 but the catalyst activity is less for an economic size of the reactor to handle
19 a higher flow rate of the feed stream, and it is mainly due to the fluidized
20 state of the catalyst bed [3]. The new design of catalyst bed with conical
21 bottom called upflow moving bed reactor (MBR) [4] solves issues pertaining
22 to hydrotreatment of heavy crude oil. The peculiarity of MBR is the conical
23 bottom attached to the catalyst bed (Figure 1), which enables the replace-
24 ment of the catalyst during hydrotreatment operation. The gas-liquid feed
25 stream is fed upflow through the MBR and maintaining the operating condi-
26 tions to keep bed expansion less than 10 percent by volume [5]. The catalyst
27 deactivates and move downward due to weight and removed from the conical
28 bottom, and then fresh or regenerated catalyst are added at the top of the
29 bed [6]. The replacement operation is not so often, and all the other times
30 the bed behaves as upflow packed or slightly expanded bed condition. The
31 successful reactor design is key to provide proper hydrodynamics, heat and
32 mass transfer conditions [7]. One of the most important design parameters
33 is liquid mixing/dispersion which is never studied for MBR reactor.

34 Inside the reactor, there is random fluctuation in the movement of the
35 phase's which is superimposed on the general flow of that phase, and it is
36 mainly due to the velocity variations and fluctuation due to varying convec-
37 tive force and bulk flow fields along the length of the reactor. This variations

and fluctuations is termed as convective dispersion/mixing of any phase and is one of the most critical hydrodynamic phenomena which directly affects mass and heat transport [8]. Hydrotreating is a liquid limited reaction and hence it is essential to understand the liquid hydrodynamics. Liquid dispersion/mixing is critical design parameter and this information is needed from bench scale/pilot scale and scaled-up to the industrial scale [2]. The dispersion/mixing is mainly due to velocity variations and fluctuations, and it is difficult to estimate the local velocities along the entire length of the reactor to quantify mixing [1]. The easier way is to conduct residence time distribution studies (RTD) for the region of interest in the reactor. Then fitting the RTD with an appropriate model having dispersion/mixing parameters to estimate it. These parameters quantify three-dimensional mixing and dispersion phenomena of liquid in the reactor.

RTD studies for the liquid phase are widely conducted on gas-liquid-solid reactor [9], but the signals are usually estimated for the entire reactor, where the liquid tracer is injected at the reactor inlet and detected at its outlet. In MBR, the area of interest is the packed bed, and RTD signals are needed for the bed section alone which is accompanied by an additional volume of plena below it and extra space on top of it. The common approach to extract the RTD signal of the bed is to employ detection of tracer below and above the volume of interest [[10], [11]], but due to the complexity of this reactor, injections are done below and top of the bed and detection is done at reactor outlet. The obtained RTDs are followed through a methodology based on

61 convolution and regression with appropriate mass transfer model describing
 62 dispersion phenomena. The most widely used model to explain the disper-
 63 sion phenomena is Axial Dispersion Model (ADM) [7], and is due to the
 64 simplicity of the ADM equation having a single parameter which accounts
 65 for the spatial complex velocity and concentration fluctuations inside the re-
 66 actor [12]. ADM is obtained by superimposing diffusional phenomena on a
 67 plug flow and based on the assumption that phase dispersion is analogous to
 68 diffusional phenomena [8]. This assumption is not valid for the cases where
 69 the velocity and timescale of the dispersion phenomena are much deviating
 70 from the time and velocity scale of the diffusion processes [12]. In two-phase
 71 packed bed reactors, the dispersion is due to the combination of various fac-
 72 tors such as velocity variations and fluctuations (Taylor dispersion), blending
 73 and separations due to flow through a tortuous path, mass exchange between
 74 stagnant and dynamic zone, molecular diffusion. The time and length scale
 75 of all these phenomena are different, and using ADM to find the dispersion
 76 phenomena fails in these cases. ADM is fundamentally second order partial
 77 diffusion equation, which has the property of infinite signal propagation [8]
 78 which necessitates the condition of applicability of ADM limited to the case
 79 of slow temporal and spatial variation of concentration field [[13] [14]]. This
 80 condition is only possible when the time scale of the transport process is
 81 extremely low and moves at infinite speed, which is the case of diffusion [[8]
 82 [12]]. For the cases, when the spatial concentration change is drastic during
 83 the time-scale of transport, such as the case when the system is noticeably

84 deviating from plug flow conditions, ADM fails. A case study is shown in
85 the section 5 below to emphasize this effect.

86 Many modifications of the ADM is found to account for various dispersion
87 causing factors in packed bed reactor. Like Piston-Exchange Model (PE)
88 model which consider stagnant and dynamic liquid zones without dispersion,
89 Piston-Dispersion-Exchange (PDE) model which accounts Dispersion also
90 [15]. These modifications are just adding up additional parameters to fit but
91 not solving the fundamental issue related to partial differential equation's
92 infinite signal propagation property which drastically limits the applicability
93 of ADM for the cases of large deviation from plug flow. To account these
94 issue [8] developed Wave Model (WM).

95 The proposed wave model by [8] consists of a set of two hyperbolic equa-
96 tion based on the simple extension of the concept formulated by [14] for
97 ADM. The one equation is for the concentration change averaged over cross
98 section and other is for the dispersion flux, the equations are shown in the
99 section 4.2. For linear problems, the equation is combined to one-second
100 order partial differential equation, which has an analytical solution. For the
101 normal pulse injection propagation of tracer in an non-reactive system, the
102 analytical solution of Wave Model is in the form of transfer function similar
103 to Gauss Jordan Distribution function [16]. The simplicity and overcom-
104 ing the conceptual difficulties of Partial Differential Equation (PDE) makes
105 Wave Model a best alternative for ADM for the limitations and conditions
106 mentioned above.

107 In this work, a liquid tracer system is developed for two-phase upflow
108 moving bed reactor (MBR), and RTD studies are conducted based on an
109 injection-sampling concept called two-point injection and one detection method.
110 The obtained RTD are processed by following a methodology based on con-
111 volution, regression and Wave Model (for catalyst bed) for estimation of
112 mixing parameter (D_l , Pe) of liquid. The results indicate the liquid mixing
113 is deviating noticeably from plug flow and a case study demonstrates that
114 ADM failed in explaining the flow behavior of liquid in the catalyst bed of
115 MBR. In addition, dimensionless variance (σ_D^2) are estimated for the bed
116 section of MBR, and it also indicates the extent of dispersion/mixing in the
117 bed section. Overall liquid dispersion/mixing is seen higher in MBR, with
118 dispersion/mixing being more in the expanded bed operating conditions.

119 2. Experimental Setup

120 The experimental setup consists of scaled down to pilot plant form in-
121 dustrial scale moving bed reactor based on matching the dynamic and geo-
122 metric similarity. The dynamic similarity is matched by keeping the pressure
123 drop same through the internal holes for both industrial and pilot scale unit.
124 Pressure drop is calculated for industrial scale at its operating condition and
125 similarly, the pressure drop is estimated at pilot plant scale at the scaled
126 down conditions. The scaled down conditions is determined by matching the
127 LHSV and gas to liquid volumetric flow rate ratio same between industrial
128 and pilot plant scale.

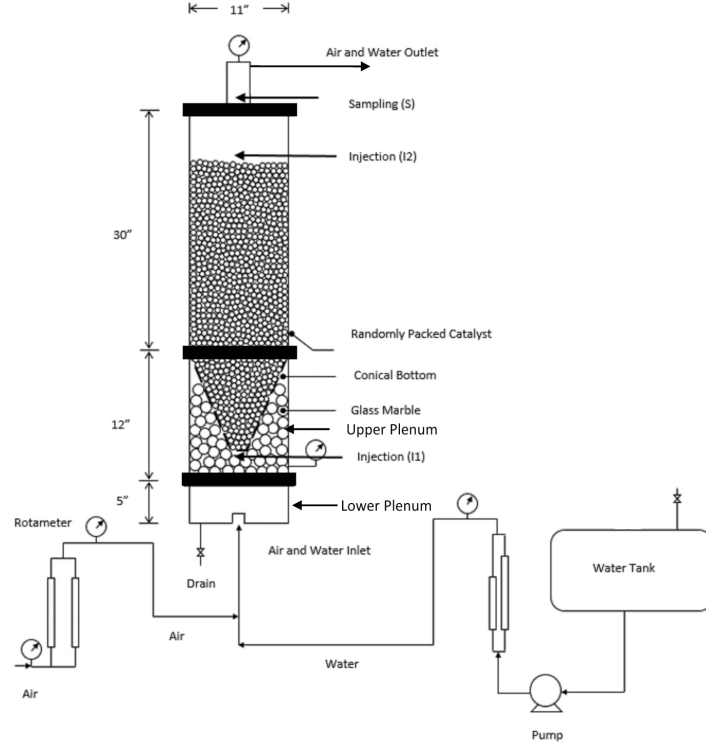


Figure 1: Schematic diagram of scaled down MBR setup for liquid dynamics studies

Figure 1 shows the schematic of the pilot scale upflow moving bed reactor (MBR). The design of this reactor is peculiar in terms of its design. It has a catalyst bed with a conical bottom, and plena classified as upper and lower plenum. The lower plenum contains deflector, 19 chimneys attached to the distributor plate in triangular pitch. Upper plenum is the compartment between the conical bottom and upper plenum wall, and this region is tightly packed with passive spheres and above the distributor plate. We conducted cold flow experimentation with gas and liquid phases as air and room temperature water. The gas phase is controlled by rotameter (Dywer-RMC-

106-SSV, Dywer-RMC-102-SSV) and the liquid phase by rotameter (Omega
FL7301, Omega FL-75C). The flow is set at desired values and fed to the re-
actor below the bottom plenum in a premixed manner. The phases enter the
reactor through the inlet of lower plenum, and it enters to the deflector which
has slots on the lateral wall. The phases are pushed out through these slots
to move upward to the chimney region. The chimneys are hollow cylindrical
pipes having a hole on its wall, these chimneys are screwed to the distributor
plate holes, such that the chimney side holes are just below the distributor
plate. At scaled down operating condition, the phases coming from the dis-
tributor will make a gas pocket formation around the chimney side hole, the
liquid will enter through the chimney bottom, and the gas will mix with the
incoming liquid phase from the side hole, and mixed phases will be sprayed
to the upper plenum. In the upper plenum, the phases will distribute due to
the packed spheres, and this mix then moves to the bed region through the
perforations on the conical bottom. Then phases will move upward through
the bed region and air-water mix coming at the outlet is sent to the drain,
as this mix will contain liquid tracer in it while conducting experimentation,
which if recycled will cause calculation error for the methodology described
in section 4.

The bed structure can change from upflow packed bed to three-phase
fluidized bed based on the flow conditions but for the scaled down operating
condition the bed is in the incipient fluidized conditions. At this state, the
bed is almost in packed bed with slight expansion at the top part of the

161 bed. In this study, we investigate the impact of flow conditions including the
 162 scaled-down conditions on liquid dispersion mixing inside the bed. Table 1
 163 shows the operating conditions and dimensions of the experimental setup.

Table 1: Experimental setup specifications and operating conditions for liquid dynamics study

Parameters	Value/Range	Comment
Column Diameter	11 inch	
Column Height	46.46 inch	
Bed Height	24.8 inch	Height from top of the cone to the top of the bed at no flow rate
Liquid (Water) Superficial Velocity	0.01 to 0.4 <i>cm/sec</i>	
Gas (Air) Superficial Velocity	1.28 to 5.13 <i>cm/sec</i>	
Scaled Down Liquid Flow Rate	0.0175 <i>cm/sec</i>	By matching LHSV of industrial and scaled down reactor
Scaled Down Gas Flow Rate	7.7 <i>cm/sec</i>	By matching Gas/liquid volumetric flow rate of industrial and scaled down reactor

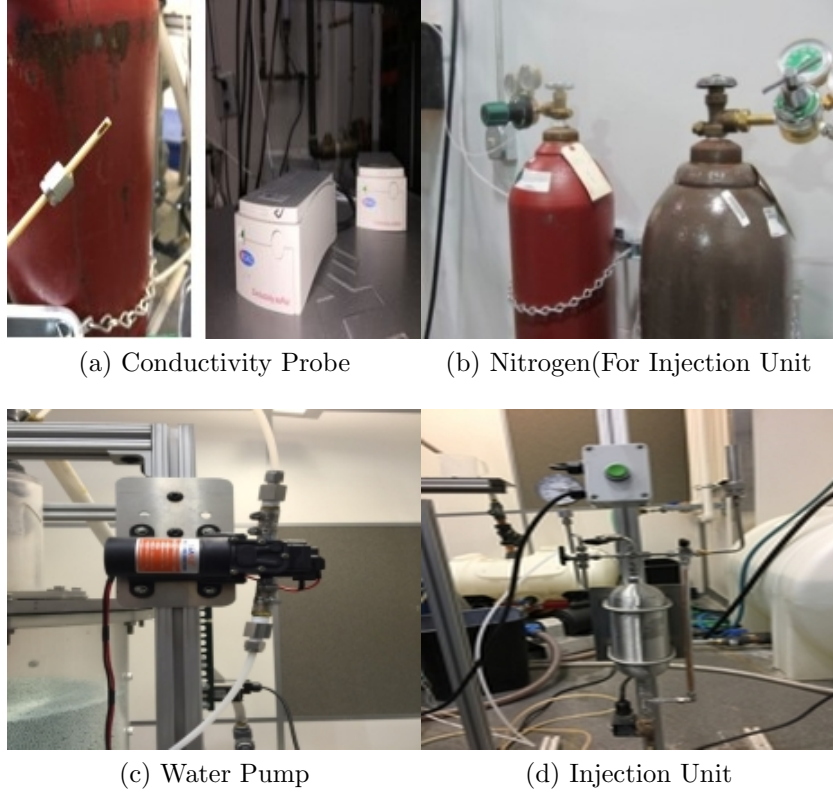


Figure 2: Liquid tracer components

164 **3. DYNAMIC LIQUID TRACER TECHNIQUE FOR RTD STUD-** 165 **IES OF LIQUID PHASE IN GAS-LIQUID UPFLOW MOVING** 166 **BED REACTOR**

167 *3.1. Dynamic Liquid Tracer Technique*

168 Figure 2 shows the component of the of the dynamic liquid tracer tech-
169 nique. KCL solution is used as the liquid tracer, after trial and error, we
170 found 1.1 M KCL solution is needed for best response with the minimum

171 of KCL for our reactor volume. KCL solution qualifies to be used as tracer
 172 as it is non-reactive, completely miscible in the liquid phase, and have the
 173 similar physical property of liquid phase [17] . The tracer is stored in an in-
 174 house developed injection unit having a cylinder and solenoid valve attached
 175 to the bottom of the cylinder (Figure 2d). The injection unit is pressurized
 176 using nitrogen gas (Figure 2b). The solenoid valve powered to open for the
 177 small amount of time using a push button, this provides a pulse injection of
 178 tracer inside the reactor. Other types of injection such as step, sinusoidal,
 179 ramp, etc. [17] can be achieved by programming the solenoid valve opening
 180 accordingly. A water pump (Figure 2c) draws the sample out from the out-
 181 let and feeds it to the conductivity probe. The Conductivity probe (Figure
 182 2a) is used to detect the tracer concentration. The probe connects to the
 183 data acquisition (edac) and samples the signal at a frequency of 25 Hz. The
 184 conductivity probe gives linear variation in the voltage signal based on the
 185 conductivity of the passing liquid. The KCL solution has higher conductiv-
 186 ity than pure water and conductivity is proportional to the concentration of
 187 KCL solution, and it is even sensitive to small traces of concentrations of
 188 KCL.

189 *3.2. Liquid Tracer System of MBR*

190 The liquid tracer system is shown in Figure 3, the system consists of two
 191 injection points (I1 and I2) and one sampling point (S). In our previous work
 192 on gas dispersion/mixing studies in upflow moving bed reactor, we used three

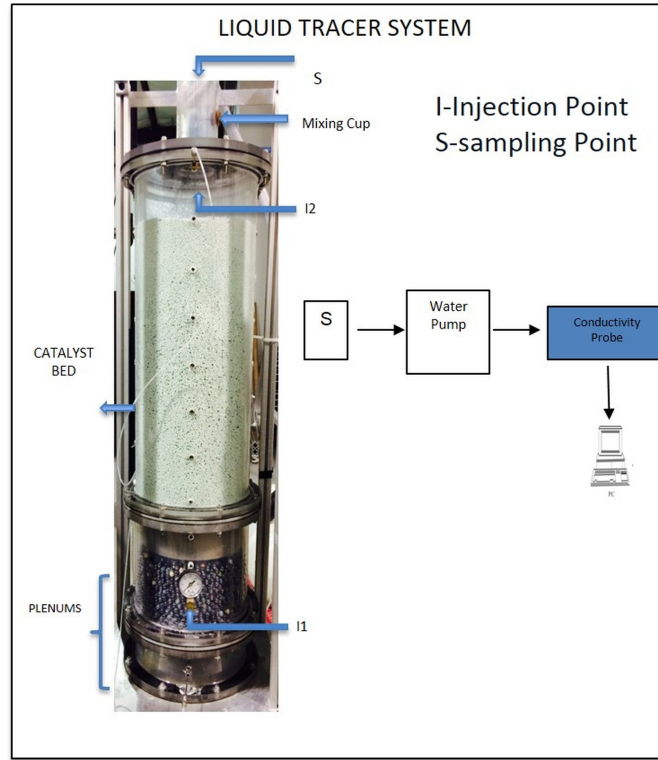


Figure 3: Liquid tracer system of MBR

193 injection and one detection [4], the different injection-sampling is due to the
 194 usage of different models and way it is solved. The methodology and models
 195 used in this study is explained in section 4. Injection points are connected
 196 to the injection unit and is the path of entry of tracer into the system.
 197 The sampling point (S) is at the outlet of the reactor and above the mixing
 198 cup, from where the gas-liquid mix is drawn out and fed to the conductivity
 199 probe using the water pump (Figure 2c). The mixing cup provides a uniform
 200 concentration cross-sectionally at the sampling plane, which is essential to
 201 neglect the effect of small tracer loss at the sampling point. Each injection

Table 2: Injection and sampling assembly for liquid dynamics study in MBR

Measurement	Injection	Sampling	Dispersion Zones
C(1)	I1	S	Zone(1): Catalystbed + Upper external Volume + Sampling Line (measurement Volume)
C(2)	I2	S	Zone(2): Upper External Volume + Sampling Line (measurement volume)

and sampling point gives the residence time distribution (RTD) of the section in between, Table 2 shows the zones covered by injection-sampling point to measure of the RTD. These assemblies of the injection/sampling are used for a method to obtain mixing parameter of the catalyst bed only and will be discussed later.

Signal Processing: The raw time series signal of tracer response is filtered using second-order butterworth filter to remove non-biased noise, such as noise due to electronics [18]. The filtered signal is normalized to a base value of zero by subtracting the signal values of filtered signal with the average signal value of the filtered signal corresponding to the air-water mixture for particular flow without any tracer. Figure 4 shows the tracer response (RTD) for injection I1-S and I2-S, the signal is again normalized to the range of 0 to 1 by dividing with maximum signal values. The shape of the RTD is dependent on the nature of flow and tracer input. For pulse input of tracer, the output response curve will be of gaussian distribution in nature and will

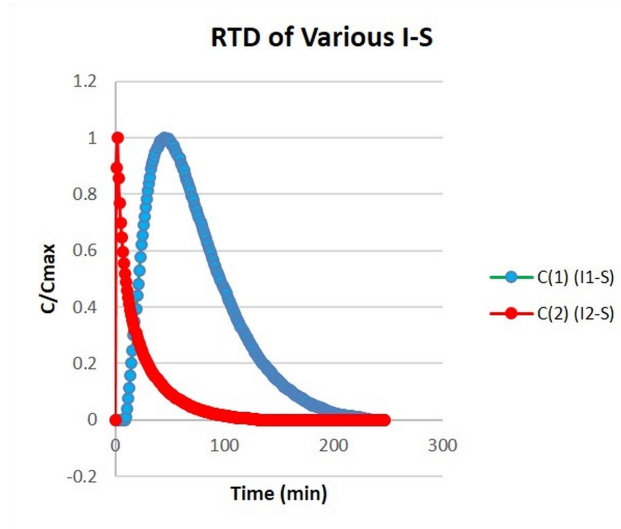


Figure 4: RTD of various injection-sampling at scaled down experimental condition

be at the extreme of the plug flow (zero dispersion) and CSTR (complete
mixing) [17].

4. Methodology To Determine Dispersion/Mixing Parameter In Catalyst Bed Section Of MBR

4.1. Two Injection and One Detection Method

The area of interest is the catalyst bed section, but the catalyst bed is
accompanied by additional volumes (Plenums, Upper extra volume, Sampling
line) as shown in Figure 3, and to exactly obtain the RTD of the bed section
we need to deconvolute the RTD signal from overall signal obtained by I-S
(Table 2). Deconvolution is numerically unstable [19] and to overcome it
we follow the methodology of single detection and multiple injection and a

228 mathematical approach of convolution and regression proposed by [19].

229 Usually two-point detection method [20], in which one injection two de-
230 tection is used to follow the convolution principle. However due to the com-
231 plexity of the MBR two-point injection and one detection is followed and
232 mathematically both yield similar results [21]. The injection is below (I1)
233 and above (I2) the catalyst bed and the detections is just above the mixing
234 cup as shown in the Figure 1. Using the RTDs obtained from the injection-
235 sampling assembly a systematic approach is followed to obtain the mixing
236 parameters. The catalyst bed section is initially modeled using an axial
237 dispersion model (ADM), but it failed to describe the dispersion/mixing be-
238 havior of liquid phase. The conceptual difficulty and explanation of its failure
239 are described as a case study in section 5. In an alternative to ADM, we used
240 a wave model (WM) to describe the liquid phase dispersion/mixing behavior,
241 which overcomes the conceptual deficiencies of ADM.

242 4.2. Wave Model

243 Wave Model is an alternative to Fickian-Type dispersion model (ADM),
244 and it overcomes some of the conceptual deficiencies of ADM [8]. It is a
245 hyperbolic system of two first order equations for the average concentration
246 (c) (equation 1) and the dispersion flux (j) (equation 2). For development of
247 model please see [8].

$$\frac{\partial c}{\partial t} + U \frac{\partial c}{\partial x} + \frac{\partial j}{\partial x} + q(c, x, t) = 0 \quad (1)$$

$$[1 + \tau \cdot q'(c, x, t)]j + \tau \frac{\partial j}{\partial t} + \tau(u + u_a) \frac{\partial j}{\partial x} = -D_e \frac{\partial c}{\partial x} \quad (2)$$

Where D_e is the Dispersion Coefficient, τ is the Relaxation time, and u_a is the Velocity Assymetry which are the parameters of the wave model. For the case of packed bed with no reaction, unit pulse injection of tracer and for arbitrary boundary condition and considering velocity asymmetry to be zero. The solution of wave model develops to gaussian distribution of the concentration as shown in equation 3.

$$C(t) = \sqrt{\frac{(-Pe * \tau)}{4 * \pi * t}} * \exp\left[\frac{-Pe * (\tau - t)^2}{4 * t * \tau}\right] \quad (3)$$

Where as Pe (peclet number) and τ (mean residence time) are the parameters. For detailed derivation of the solution of the wave model refers to [8] and [16].

$$PecletNumber(Pe) = \frac{U * L}{\epsilon_l * D_L} \quad (4)$$

Essentially the parameter of the solutions are ϵ_l (liquid holdup), D_l (Liquid dispersion), τ is equivalent to t_m (mean residence time), U (superficial velocity), and L (Length of the packed bed) This Gaussian function [16] relates the concentration at one position to that at another location with the degree of longitudinal mixing governed by Pe . This transfer function is used in this study to evaluate liquid behavior in the bed at the flowing conditions by estimating its parameters mentioned above.

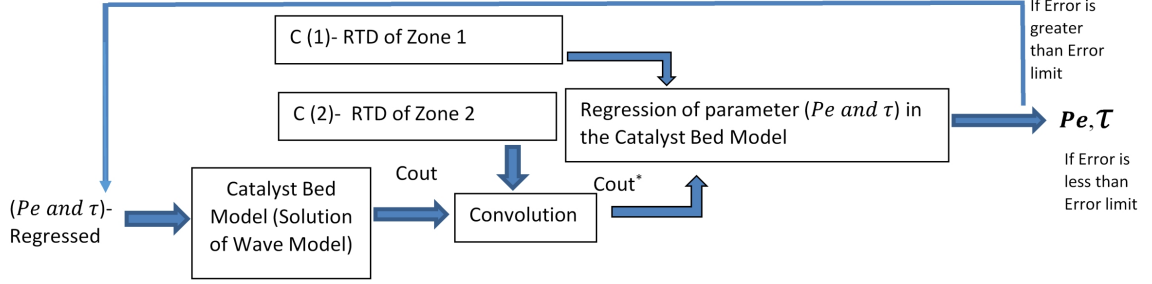


Figure 5: Schematic of convolution and regression approach to obtain liquid mixing parameters of catalyst bed

4.3. Convolution and Regression Approach to Estimate Liquid Dispersion Coefficient (D_l) and Peclet Number (Pe) of Liquid Phase in Catalyst Bed Section of MBR

Pe and τ values are assumed initially and fed into equation 3 and the resulting output C_{out} (Figures 5 and 6) represents the solution for unit pulse input of tracer at the outlet of the catalyst bed. Convolution Principle is applied using equation 5. C_{out} is input to zone-2 and C(2) (Figure 5 and 6) is the experimental response of zone 2. The output C_{out*} (Figures 5 and 6) represents the output from zone 2 for an inlet response of C_{out} which itself is the outlet of catalyst bed for unit pulse injection. Hence, C_{out*} is theoretical output of catalyst bed section plus zone-2, which is equivalent to zone 1. It means C_{out*} is theoretical output of Zone-1.

$$C_{out*} = \int_0^t C_{out}(t') \cdot C_2(t - t') \cdot dt' \quad (5)$$

Estimation of Pe and τ : C(1) (Figure 7) represents the experimental

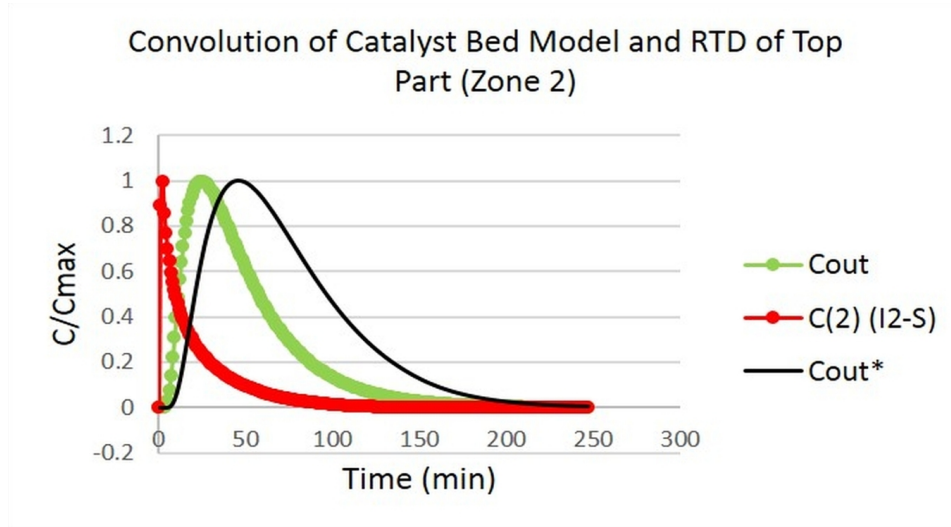


Figure 6: C_{out} (solution of the wave Model), $C(2)$ (experimental output of zone-2), C_{out}^* (convoluted signal of C_{out} and Zone-2), at the experimental scaled down conditions

277 output of zone 1 and C_{out}^* (Figure 7) represents the theoretical output of
 278 Zone 1 based on the solution of Wave Model for parameter Pe and τ . $C1$
 279 and C_{out}^* are regressed using equation(6) for minimum error for the values of
 280 Pe and τ . These values represent the actual model parameters for equation
 281 (3) representing the liquid phase flow behavior inside the catalyst bed.

$$Error = \frac{1}{n} \sum_{j=1}^n [C_{out}^*(t_j) - C(1)(t_j)]^2 \quad (6)$$

282 The minimum averaged sum of square error (equation 6) value for the case
 283 shown in Figure 7 is 0.00013, this validates that Wave Model is applicable to
 284 quantify liquid flow dynamics in catalyst bed section of MBR. The estimated
 285 parameter are $Pe=3.78$, and $\tau=32$ min.

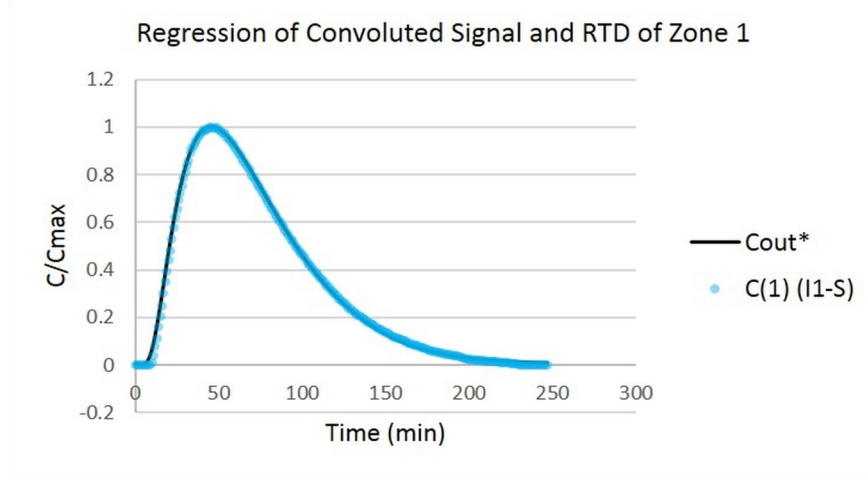


Figure 7: The regression plot for minimum error between convoluted signal (C_{out*}) and experimental response $C(1)$, at experimental scaled down condition

286 Estimation of D_l : The D_l is calculated using the equation 4, where the
 287 unknown is ϵ_l , and rest of all the quantities are known. ϵ_l can be estimated
 288 using the equation 7 and equation 9 based on RTD response [3].

$$\epsilon_{l1} = \frac{V_L}{X} * t_{m1} \quad (7)$$

289 Where ϵ_{l1} is the liquid holdup of zone1, V_L is the superficial liquid velocity
 290 based on empty column, X is the linear distance of zone 1, and t_{m1} is the mean
 291 residence time calculated using equation 8 for the RTD of Zone 1 ($C(1)$).

$$t_{m1} = \frac{\int C(1).t}{\int C(1)} \quad (8)$$

$$\epsilon_{l2} = \frac{V_L}{Y} * t_{m2} \quad (9)$$

Where ϵ_{l2} is the Liquid holdup of zone-2, V_L is the superficial liquid velocity based on empty column, Y is the linear distance of zone-2, and t_{m2} is the mean residence time calculated using equation 10 for the RTD of zone-2 ($C(2)$).

$$t_{m2} = \frac{\int C(2).t}{\int C(2)} \quad (10)$$

now using the equation

$$\epsilon_L = \frac{VolumeofLiquidinBed}{VolumeofBed} = \frac{\epsilon_{L1} * V_{zone1} - \epsilon_{L2} * V_{zone2}}{V_{catalystbed}} \quad (11)$$

In equation 11, all the terms (ϵ_{l1} , ϵ_{l2}) are known from equation 7 and equation 9, and V_{zone1} , V_{zone2} , and $V_{catalystbed}$ are known from reactor geometry. The estimated $D_l = 0.0065 \text{ m}^2/\text{min}$ for the experimental scaled down condition.

5. Case Study to show failure of ADM

The methodology shown in section 4 is applied with replacing the model of catalyst bed with Axial Dispersion Model (ADM) for Dirac delta input as shown in Figure 8.

C_{out} is the solution of the ADM which is input to the zone-3. The same convolution principle of equation (5) is applied and C_{out*} is obtained. The C_{out*} represents the theoretical output of zone-1 and $C(1)$ represents the experimental output of zone-1. The C_{out*} and $C(1)$ are regressed for D_l and

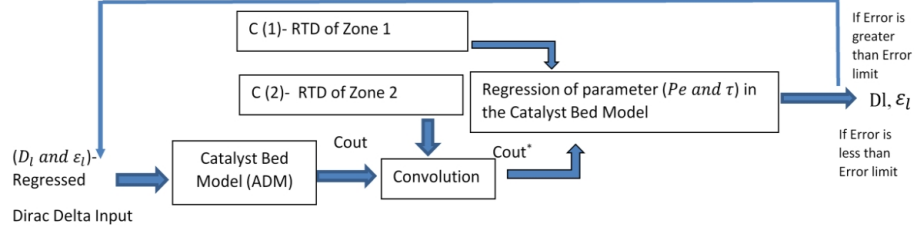


Figure 8: Schematic of convolution and regression approach using ADM model for catalyst bed

308 ϵ_l for minimum error using the equation 6.

$$\frac{\partial C_L}{\partial t} = D_l \frac{\partial^2 C_L}{\partial Z^2} - \frac{U_L}{\epsilon_L} \frac{\partial C_L}{\partial Z} \quad (12)$$

Boundary Conditions:

$$Z = 0, U_g.C_{in} = U_L.C_L|_{z=0} - D_l \frac{\partial C_L}{\partial Z}|_{z=0} \quad (13)$$

$$Z = L, \frac{\partial C_L}{\partial z}|_{z=L} = 0 \quad (14)$$

309 Figure 9 shows the regression plot for the theoretical output using ADM
 310 and Experimental Output of RTD for Zone-1. The plots show the best
 311 regression possible for least error of 0.125. The least error is much higher
 312 than the tolerance limit for good fit (max error of 0.005), whereas using
 313 Wave Model for same operating conditions, the error was 0.00035 within
 314 the tolerance (Figure 7). This indicates, ADM is not a suitable model for
 315 liquid phase dispersion studies in catalyst bed section of this reactor. On
 316 carefully analyzing the Figure 9, one can see that theoretical output has

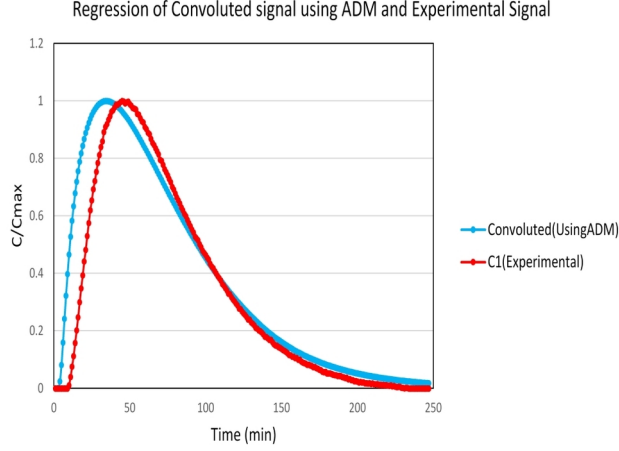


Figure 9: The regression plot for minimum error between convoluted signal (using ADM) and experimental response $C(1)$, at scaled down experimental conditions

317 signal value at a time from (0 min), whereas for the experimental output,
 318 the first signal value is at (3min), This is the primary reason for the non-
 319 fit condition between theoretical and experimental output. Why theoretical
 320 output generates a signal at zero time is due to the fundamental nature of
 321 ADM equation. ADM is second order parabolic differential equation, and the
 322 solution of these equations have an infinite speed of signal propagation, which
 323 means instantaneous signal (concentration) at all the modeling space with
 324 the intensity proportional to dispersion coefficient [8]. ADM can be better
 325 understood by focusing on ficks law, based on which ADM is conceived.

326 Westerterp ([12]) analyzed the ficks law for diffusional phenomena at par-
 327 ticle level scrutiny and found that, to hold ficks law, the time taken (relax-
 328 ation time) for random particle movement (mean free path) shall approach
 329 zero. Hence, the velocity scale (mean free path/relaxation time) of diffu-

330 sional transport shall approach infinity. Hence, ADM is applicable for the
 331 cases when these conditions are fulfilled or not much deviating from it, or
 332 it is only properly applicable for the case of molecular diffusion, as infinite
 333 velocity scale of molecular diffusion justifies physically the ADM behavior
 334 of infinite signal propagation [22]. The cases, such the flow of gas phases,
 335 the relaxation time of particle movement is very slow to the order of (10^{-10}
 336 to 10^{-11} sec) which is comparable with the diffusional time scale, and hence
 337 ADM is applicable for gas phase with a reasonable level of accuracy [8]. The
 338 liquid phase flow has a time scale of particle movement higher than the dif-
 339 fusional phenomena and hence not reasonable to use ADM to find dispersion
 340 phenomena.

341 **6. Dimensionless Variance (Tank in Series)**

342 Tank in series is a one parameter model and are used to describe non-ideal
 343 reactors. In this modeling concept, n tanks are modeled as ideal CSTR in
 344 series for pulse injection of tracer. The Residence Time Distribution (RTD)
 345 obtained from the model is matched with experimental RTD of non-ideal
 346 reactor by varying n. Larger the value of n indicating the flow is towards
 347 plug flow and lower means the flow is towards CSTR. Fogler ([23]) showed
 348 that equation 15 is the generalized RTD for n tank modeled as ideal CSTR
 349 in series.

$$E(t) = \frac{t^n}{(n-1)!\tau_i^n} e^{-t/\tau_i} \quad (15)$$

Where τ_i is the means residence time in single tank, n is the number of tank, and τ_i is equal to τ/n , and τ is mean residence time of entire reactor. Equation 15 is converted to dimensionless form $E(\theta)$ as shown in Equation 16.

$$E(\theta) = \tau E(\theta) = \frac{n(n\theta)^{n-1}}{(n-1)!} e^{-n\theta} \quad (16)$$

Where θ is the ratio of t and τ . The variance of equation 16 can be found using equation 17, which is called dimensionless variance (σ_D^2), and this dimensionless variance is equal to the ratio of variance (σ^2) and square of mean residence time (t_m).

$$\sigma_D^2 = \frac{\sigma^2}{t_m^2} = \int_0^\infty (\theta - 1)^2 E(\theta) d\theta \quad (17)$$

[23] showed the solution of equation 17 is equal to the inverse of number of tanks (n), as shown in equation 18.

This indicates if σ_D^2 is zero then the flow is towards the plug flow as n tends to infinite ideal CSTR in series, and when σ_D^2 approaches one the flow is towards complete mixing as n tends to one ideal CSTR . Dimensionless variance can be determined by RTD experiments, as it is the ratio of variance (σ^2) (second moment) and square of mean residence time (t_m) (first moment).

$$\sigma_D^2 = \frac{\sigma^2}{t_m^2} = \frac{1}{n} \quad (18)$$

$$MeanResidenceTime(t_m) = \int_0^{\infty} E(t)tdt \quad (19)$$

$$Variance(\sigma^2) = \int_0^{\infty} (t - t_m)^2 E(t)dt \quad (20)$$

365 In our case, the area of interest is packed bed region, and its dimensionless
 366 variance is evaluated by finding the variance of RTD of zone 1 (t_{m1}) (Figure
 367 4 and Table 2) and RTD of zone 2 (t_{m2}) (Figure 4 and Table 2) using the
 368 equation 19 and similarly the variance (σ_1^2 and σ_2^2) using equation 20. Volume
 369 of Zone 1 minus volume of zone 2 gives volume of bed , and as these moments
 370 are additive the bed variance will ($\sigma_1^2 - \sigma_2^2$) and mean residence time in the
 371 bed will be ($t_{m1} - t_{m2}$). Hence the σ_D^2 is calculated using equation 21.

$$\sigma_D^2(Bed) = \frac{(\sigma_1^2 - \sigma_2^2)}{(t_{m1} - t_{m2})^2} \quad (21)$$

372 Equation 21 shows the dimensionless variance of the liquid phase in cat-
 373 alyst bed region and for scaled down experimental condition (Table 1), σ_D^2
 374 is 0.331.

375 7. Results and Discussion

376 The evaluated wave model (WM) parameters are liquid dispersion co-
 377 efficient (D_l) and Peclet number (Pe). In addition, dimensionless variance
 378 (σ_D^2) in the bed region is evaluated. These parameters estimate the extent
 379 of mixing of liquid phase in catalyst bed section of this reactor. The effect

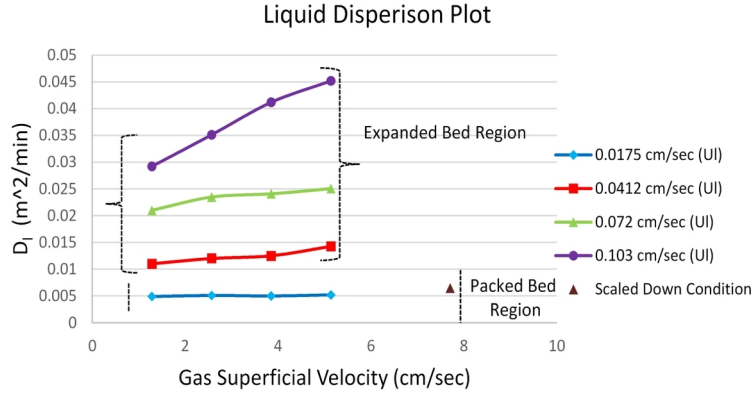


Figure 10: The liquid dispersion in the catalyst bed of MBR for varying flow rate of phases

of operating conditions on these parameters are investigated.

7.1. Effect of Operating Condition on Dispersion Inside the Catalyst Bed Section of MBR

The physical representation of D_l is the quantification of the spread of tracer signal in the catalyst bed section. The spreading is dependent on diffusive nature of tracer and spread occurring due to the external force field which is dependent on the flow condition. Hence, the dispersion coefficient (D_l) can be represented as the summation of molecular diffusivity and dispersion due to convective term [9]. Any non-ideality in the flow is reflected in the convective dispersion term. The primary source of non-ideality for liquid flow in two-phase upflow packed or expanded bed are due to non-uniform velocity profile, by passing streams of phases, velocity fluctuations due to turbulence, backflow of liquid due to velocity difference with gas phase, non-uniform flow pattern of gas phase in bed, mass transfer between dynamic and

394 stagnant liquid zones [24]. All these non-idealities are a function of reactor
 395 design, bed structure and operating condition of phases. Figure 10 shows
 396 the effect of gas and liquid superficial velocity on the liquid dispersion in the
 397 catalyst bed packing of this reactor. Based on the operating condition the
 398 bed structure changes from packed bed to expanded. The previous study
 399 of ([4]) indicates that for liquid flow rate (0.0175 cm/sec) and varying gas
 400 flow rate from (1 to 7 cm/sec), the bed is in packed condition, with slight
 401 expansion at the top for scaled down conditions (Table 1). For the rest of all
 402 the operating conditions the bed starts to expand, and its extent depends on
 403 flow condition. The dispersion trend of liquid is seen different for the packed
 404 bed and expanded bed case. In packed bed case (Figure 10) the liquid dis-
 405 persion is not changing significantly with increasing flow rate of gas and the
 406 same observed by [11]. In packed bed region with increase in gas flow the
 407 bubble breakup phenomena increases and moves upwards as small bubbles,
 408 these small rising bubbles cause less dispersion/mixing in liquid [25]. Other
 409 main criteria which can induce non-ideality or increased spreading of liquid
 410 are liquid flow rates and bed structure, where the bed structure is not much
 411 changing for all the operating condition in packed bed case. In expanded
 412 bed case the situation changes as the bed structure changes with operating
 413 conditions.

414 The operating region of expanded bed is shown in Figure 10. In this
 415 region, the bed starts to expands and moves toward three phase fluidization.
 416 It is seen that for all liquid flow rates the liquid dispersion coefficient (D_l) is

417 increasing with increase in gas flow rate. A similar trend is observed by [7]
 418 for three-phase fluidized bed. It is also seen that D_l increases with increase
 419 in liquid flow rate and the increasing effect with respect to increase in the gas
 420 flow is greater for higher liquid flow rates. The extent of the bed expansion is
 421 proportional to the increase in the flow rate of phases for MBR ([4]). With in-
 422 creasing liquid flow rate the bed expansion increases which result in increase
 423 liquid spreading induced by moving solids. In expanded bed, with increas-
 424 ing gas flow rate results in bubble coalescence, channeling and random flow
 425 distribution of gas phase along the bed, which increases the bubble-induced
 426 turbulence and macro recirculation of liquid phase [7]. These phenomena
 427 increase dispersion of liquid phase in expanded bed region. From the results,
 428 it is indicative that the liquid dispersion is a strong function of flow rate of
 429 phases and its effect is intense for a higher flow rate of phases. Although this
 430 gives good trend to understand the dispersive nature but to identify nature
 431 of flow such as pulse flow or completely mixed, a peclet number is needed.
 432 As the calculated D_l is proportional to the convective component of liquid
 433 phase flow, and its increase will result in increasing trend of D_l , but it does
 434 not mean the flow is moving toward completely mixed flow. Hence, the com-
 435 parison of bulk flow field with dispersive force field is done by finding the
 436 peclet number (Pe).

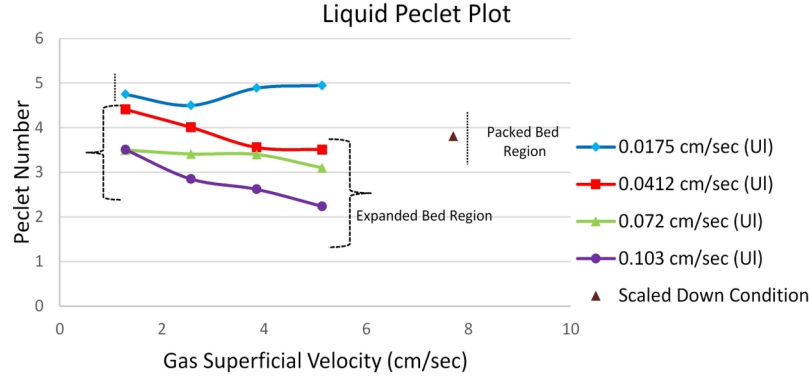


Figure 11: The liquid peclet number in catalyst bed of MBR for varying flow rate of phases

7.2. Effect of Operating Conditions on Peclet Number Inside the Catalyst Bed Section of MBR

Peclet (Pe) number is calculated using the equation 4, and it indicates whether advective or dispersive field dominates the nature of the flow. Higher the Pe , flow is towards the plug flow, and for lower Pe the flow is towards complete mixing. Figure 11 shows the peclet number plot for the liquid phase for the varying flow rate of phases. The plot shows that for both packed bed and expanded bed region, the Pe number is decreasing with increasing flow rate of gas phase and liquid phase, the decrease of Pe with increasing gas flow rate is more significant at higher liquid flow rates. For packed and slightly expanded bed cases the Pe for liquid is seen to decrease with gas flow rate [[2], [20], [26], [1]]. The small values of the peclet number clearly indicate that liquid phase non-ideality is quite significant and largely deviating from the plug flow [[9], [27]]. These non-idealities are much dominant in expanded

451 bed case, and is seen to be increasing function with bed expansion.

452 As the bed expands, dispersion of liquid phase increases as explained in
453 the section 7.1. At expanded bed conditions the bubble coalescence and
454 other maldistribution and catalyst particle movement is observed. These
455 movement creates a force field for micro and macro recirculation zones in the
456 bed for liquid phase [28]. These recirculations increases the residence time
457 of the liquid phase and results in dominance of dispersive forces compared
458 to convective. The dispersive forces are directly linked with hydrodynamics
459 mixing which includes backmixing and thus decreases Pe with increasing
460 liquid flow rate. For MBR at the hydrotreating condition, the condition
461 of low bed expansion is preferable for maximum catalyst utilization [5]. In
462 terms of liquid mixing the scaled down conditions are suitable, as based on its
463 low Pe value the mixing is already quite good. Pe gives a good indication of
464 mixing phenomena in the bed, but additionally, dimensionless variance (σ_D^2)
465 is evaluated using the moments of experimental RTDs, as this parameter is
466 also indicates the degree of dispersion/mixing.

467 *7.3. Effect of Operating Conditions on Dimensionless Variance Inside the* 468 *Catalyst Bed Section of MBR*

469 The dimensionless variance (σ_D^2) indicates the degree of dispersion/mixing
470 in the reactor. The procedure to calculate σ_D^2 is shown in section 6. If the
471 values of σ_D^2 is zero it indicates the flow is in plug flow and if its one then
472 flow is completely mixed. Figure 12 shows the dimensionless variance plot

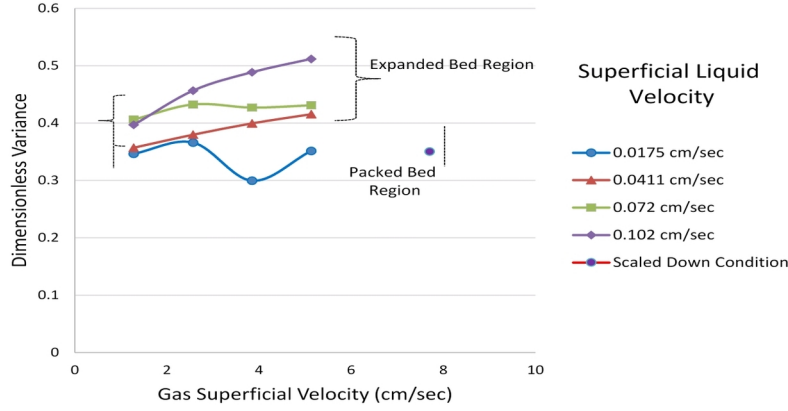


Figure 12: The liquid dimensionless variance in catalyst bed of MBR for varying flow rate of phases

for varying flow rate of phases and at scaled down conditions. The results indicates similar dispersion/mixing behavior of liquid phase in the bed as we observed with peclet plot (Figure 11). For packed bed the σ_D^2 is slightly increases with gas velocity, indicating gas phase doesnt have significant effect on liquid dispersion/mixing at these conditions. At expanded bed condition the σ_D^2 is increasing with increasing flow rate of both the phases. This indicates the dispersion or mixing is increasing and going towards complete mixing in the expanded bed case and is a direct function of bed expansion. The value of σ_D^2 is in the range of 0.3 to 0.52 indicating noticeable deviation from plug flow behavior, as σ_D^2 value of around 0.1 or less is considered to be in plug flow [29]. Scaled down experimental condition shows a σ_D^2 value of 0.33 showing high dispersion/mixing of liquid phase at these conditions, and at these conditions the bed behaves as upflow packed with slight expansion,

486 which is needed for better catalyst utilization.

487 8. Remarks

488 Liquid phase dispersion/mixing is successfully investigated for the first
489 time in the catalyst bed of upflow moving bed reactor (MBR) using residence
490 time distribution (RTD) studies. The catalyst bed is modeled using Wave
491 Model (WM), and its dispersion or mixing parameters (D_l and Pe) are esti-
492 mated using a mathematical approach based on convolution and regression.
493 A case study is also shown to illustrate the limitation of Axial Dispersion
494 Model (ADM) for modeling the liquid phase flow behavior in MBR. In ad-
495 dition, a dimensionless variance (σ_D^2) in the bed section is estimated using
496 the first moment (t_m) and second moment (σ^2) of the experimental RTD.
497 The D_l result indicates the liquid dispersion is not much affected by the in-
498 crease in gas flow rate in packed bed region, but in expanded bed regions
499 D_l increases with increasing flow rate of both the phases and is due to the
500 increase in bed expansion with flow rate. Pe and σ_D^2 showed that overall
501 liquid dispersion/mixing is higher in MBR for all the operating conditions
502 studied, but mixing/dispersion is more in expanded bed and increases with
503 bed expansion. The value of Pe and σ_D^2 also indicates that the liquid flow is
504 noticeably deviating from plug flow and moving towards completely mixing
505 with bed expansion. For hydrotreatment application in MBR, scaled down
506 conditions are preferable, as the Pe and σ_D^2 indicates high liquid mixing,
507 and moreover, at these conditions, the bed behavior is in upflow packed with

508 slight expansion at the top, which is a necessary condition for good catalyst
509 utilization.

510 9. Acknowledgments

511 The authors like to acknowledge the financial and technical support given
512 by the Kuwait Institute for Scientific Research (KISR), Kuwait National
513 Petroleum Company (KNPC), and Kuwait Petroleum Corporation (KPC).
514 Binbin Qi for facilitating the submission of this article to journal.

- 515 [1] I. Iliuta, F. C. Thyron, O. Muntean, Axial dispersion of liquid in gas-
516 liquid cocurrent downflow and upflow fixed-bed reactors with porous
517 particles, *Chemical Engineering Research and Design* 76 (1998) 64–72.
- 518 [2] A. M. Thanos, P. A. Galtier, N. G. Papayannakos, Liquid dispersion
519 and holdup in a small-scale upflow hydrotreater at high temperatures
520 and pressure, *Chemical Engineering Science* 56 (2001) 693–698.
- 521 [3] S. Kressmann, C. Boyer, J. J. Colyar, J. M. Schweitzer, J. C. Viguie,
522 Improvements of ebullated-bed technology for upgrading heavy oils, *Oil
523 and Gas Science and Technology* 55 (2000) 397–406.
- 524 [4] V. Alexander, H. Albazzaz, M. Al-Dahhan, Gas phase dispersion/mixing
525 investigation in a representative geometry of gas-liquid upflow moving
526 bed hydrotreater reactor (mbr) using developed gas tracer technique and
527 method based on convolution/regression, *Chemical Engineering Science*
528 195 (2019) 671 – 682.

- 529 [5] D. C. Kramer, B. E. Stangeland, D. S. Smith, J. T. McCall, G. L.
530 Scheuerman, R. W. Bachtel, Apparatus for an on-stream particle re-
531 placement system for countercurrent contact of a gas and liquid feed
532 stream with a packed bed, US Patent, US5302357A (1994).
- 533 [6] W. B. Krantz, D. E. Earls, H. J. Trimble, J. Chabot, K. Parimi, Bal-
534 anced flow resistance OCR distributor cone, US Patent, US6387334B1
535 (2002).
- 536 [7] K. Muroyama, L.-S. Fan, Fundamentals of gas-liquid-solid fluidization,
537 AIChE Journal 31 (1985) 1–34.
- 538 [8] K. R. Westerterp, V. V. Dil’man, A. E. Kronberg, Wave model for
539 longitudinal dispersion: Development of the model, AIChE Journal 41
540 (1995) 2013–2028.
- 541 [9] J. M. P. Q. Delgado, A critical review of dispersion in packed beds, Heat
542 and Mass Transfer/Waerme- und Stoffuebertragung 42 (2006) 279–310.
- 543 [10] M. Edwards, J. Richardson, Gas dispersion in packed beds, Chemical
544 Engineering Science 23 (1968) 109 – 123.
- 545 [11] L. Valenz, F. J. Rejl, V. Linek, Gas and liquid axial mixing in the
546 column packed with Mellapak 250Y, Pall rings 25, and intalox saddles
547 25 under flow conditions prevailing in distillation columns, Industrial
548 and Engineering Chemistry Research 49 (2010) 10016–10025.

- 549 [12] K. R. Westerterp, A. E. Kronberg, A. H. Benneker, V. V. Dil'man,
550 Wave concept in the theory of hydrodynamical dispersion a Maxwellian
551 type approach, *Chemical Engineering Research and Design* 74 (1996)
552 944–952.
- 553 [13] P. Danckwerts, Continuous flow systems: Distribution of residence
554 times, *Chemical Engineering Science* 2 (1953) 1 – 13.
- 555 [14] G. I. Taylor, Diffusion and mass transport in tubes, *Proceedings of the*
556 *Physical Society. Section B* 67 (1954) 857.
- 557 [15] A. Beg, M. Hassan, M. Naqvi, Hydrodynamics and mass transfer in
558 a cocurrent packed column a theoretical study, *Chemical Engineering*
559 *Journal and the Biochemical Engineering Journal* 63 (93-103) 1–2.
- 560 [16] A. H. Benneker, A. E. Kronberg, J. W. Post, A. G. J. Van Der Ham,
561 K. R. Westerterp, Axial dispersion in gases flowing through a packed
562 bed at elevated pressures, *Chemical Engineering Science* 51 (1996) 2099–
563 2108.
- 564 [17] Y. T. Shah, G. J. Stiegel, M. M. Sharma, Backmixing in gas-liquid
565 reactors, *AIChE Journal* 24 (1978) 369–400.
- 566 [18] M. H. Al-Dahhan, P. L. Mills, P. Gupta, L. Han, M. P. Dudukovic, T. M.
567 Leib, J. J. Lerou, Liquid-phase tracer responses in a cold-flow counter-
568 current trayed bubble column from conductivity probe measurements,

- 569 Chemical Engineering and Processing: Process Intensification 45 (2006)
570 945–953.
- 571 [19] L. Han, Hydrodynamics and mass transfer in slurry bubble column, PhD
572 Thesis, 2007.
- 573 [20] M. C. Cassanello, O. M. Martinez, A. L. Cukierman, Effect of the
574 liquid axial dispersion on the behavior of fixed bed three phase reactors,
575 Chemical Engineering Science 47 (1992) 3331–3338.
- 576 [21] N. Midoux, J. C. Charpentier, On an experimental method of residence
577 time distribution measurement in the fast flowing phase of a two-phase
578 flow apparatus: Application to gas flow in gas-liquid packed column,
579 The Chemical Engineering Journal 4 (1972) 287–290.
- 580 [22] A. A. Iordanidis, M. van Sint Annaland, A. E. Kronberg, J. A. M.
581 Kuipers, A critical comparison between the wave model and the stan-
582 dard dispersion model, Chemical Engineering Science 58 (2003) 2785–
583 2795.
- 584 [23] H. S. Fogler, Elements of chemical reaction engineering 4th Edition
585 (2005).
- 586 [24] I. Iliuta, F. C. Thyron, O. Muntean, Hydrodynamic characteristics of
587 two-phase flow through fixed beds: Air/newtonian and non-newtonian
588 liquids, Chemical Engineering Science 51 (1996) 4987–4995.

- 589 [25] L. Belfares, M. Cassanello, B. P. A. Grandjean, F. Larachi, Liquid back-
590 mixing in packed-bubble column reactors: A state-of-the-art correlation,
591 Catalysis Today 64 (2001) 321–332.
- 592 [26] L. Xie, Z. Li, H. Liu, Axial dispersion and pressure drop of a slightly
593 expanded bed reactor, Beijing Huagong Daxue Xuebao (Ziran Kex-
594 ueban)/Journal of Beijing University of Chemical Technology (Natural
595 Science Edition) 40 (2013) 1–7.
- 596 [27] R. S. Abdulmohsin, M. H. Al-Dahhan, Axial dispersion and mixing
597 phenomena of the gas phase in a packed pebble-bed reactor, Annals of
598 Nuclear Energy 88 (2016) 100–111.
- 599 [28] A. K. Saroha, R. Khera, Hydrodynamic study of fixed beds with cocur-
600 rent upflow and downflow, Chemical Engineering and Processing: Pro-
601 cess Intensification 45 (2006) 455–460.
- 602 [29] D. Tang, J. A., R. X., B. B., S. S., Axial dispersion and wall effects in
603 narrow fixed bed reactors: A comparative study based on rtd and nmr
604 measurements, Chemical Engineering & Technology 27 (2004) 866–873.